5930–5944 *Nucleic Acids Research, 2017, Vol. 45, No. 10* *Published online 28 April 2017*
doi: 10.1093/nar/gkx317

Identification of miRNA-7 by genome-wide analysis as a critical sensitizer for TRAIL-induced apoptosis in glioblastoma cells

Xiao Zhang[1,†], Xiang Zhang[1,†], Shijie Hu[2,†], Minhua Zheng[3], Jie Zhang[4], Jianhui Zhao[2], Xiaofang Zhang[1], Bo Yan[1], Lintao Jia[1], Jing Zhao[1], Kaichun Wu[5], Angang Yang[6,*] and Rui Zhang[1,*]

[1]The State Key Laboratory of Cancer Biology, Department of Biochemistry and Molecular Biology, The Fourth Military Medical University, Xi'an, Shaanxi 710032, P.R. China, [2]Department of Neurosurgery, Xijing Hospital, The Fourth Military Medical University, Xi'an, Shaanxi 710032, P.R. China, [3]The State Key Laboratory of Cancer Biology, Department of Medical Genetics and Developmental Biology, The Fourth Military Medical University, Xi'an, Shaanxi 710032, P.R. China, [4]Department of Radiological Medicine, The Fourth Military Medical University, Xi'an, Shaanxi 710032, P.R. China, [5]The State Key Laboratory of Cancer Biology and Xijing Hospital of Digestive Diseases, Xijing Hospital, The Fourth Military Medical University, Xi'an, Shaanxi 710032, P.R. China and [6]The State Key Laboratory of Cancer Biology, Department of Immunology, The Fourth Military Medical University, Xi'an, Shaanxi 710032, P.R. China

Received January 08, 2017; Revised March 28, 2017; Editorial Decision April 12, 2017; Accepted April 18, 2017

ABSTRACT

Glioblastoma (GBM) is still one of the most lethal forms of brain tumor despite of the improvements in treatments. TRAIL (TNF-related apoptosis-inducing ligand) is a promising anticancer agent that can be potentially used as an alternative or complementary therapy because of its specific antitumor activity. To define the novel pathways that regulate susceptibility to TRAIL in GBM cells, we performed a genome-wide expression profiling of microRNAs in GBM cell lines with the distinct sensitivity to TRAIL-induced apoptosis. We found that the expression pattern of miR-7 is closely correlated with sensitivity of GBM cells to TRAIL. Furthermore, our gain and loss of function experiments showed that miR-7 is a potential sensitizer for TRAIL-induced apoptosis in GBM cells. In the mechanistic study, we identified XIAP is a direct downstream gene of miR-7. Additionally, this regulatory axis could also exert in other types of tumor cells like hepatocellular carcinoma cells. More importantly, in the xenograft model, enforced expression of miR-7 in TRAIL-overexpressed mesenchymal stem cells increased apoptosis and suppressed tumor growth in an exosome dependent manner. In conclusion, we identify that miR-7 is a critical sensitizer for TRAIL-induced apoptosis, thus making it as a promising therapeutic candidate for TRAIL resistance in GBM cells.

INTRODUCTION

Glioblastoma multiforme (GBM) is the most aggressive form of brain tumors, with a median survival time no more than 16 months. Despite considerable advances in GBM therapy, it remains one of the most challenging diseases. Intrinsic resistance to apoptosis is one of the most critical obstacles for the clinical treatment (1). Recently, an increasing number of studies have demonstrated that directly targeting primary tumor masses or even metastatic lesions by genetically modified mesenchymal stem cells (MSCs) with therapeutic agents could be a promising therapeutic approach (2).

Tumor necrosis factor (TNF)-related apoptosis-inducing ligand (TRAIL) is a member of the TNF superfamily (TNFSF). TRAIL gained much attention during the past decade due to its therapeutic potential as a tumor-specific apoptosis inducer without affecting normal cells (3–5). A growing number of evidences demonstrated that TRAIL itself as well as agonists of the two human receptors of TRAIL which can transfer the extracellular death signal, TRAIL-R1 (DR4) and TRAIL-R2 (DR5) is a novel biotherapeutics for cancer therapy (6,7). However, the clinical application of recombinant TRAIL, have been hampered

*To whom correspondence should be addressed. Tel: +86 29 84776799; Fax: +86 29 84773947; Email: ruizhang@fmmu.edu.cn
Correspondence may also be addressed to Angang Yang. Tel: +86 29 84774528; Fax: +86 29 83253816; Email: agyang@fmmu.edu.cn
†These authors contributed equally to the paper as first authors.

by its short half-life and unstable property *in vivo*. To overcome its limited efficacy, genetically modified MSCs with high levels of TRAIL expression have been used to specifically delivery TRAIL to tumor tissues. It has partially counteracted the shortcoming of TRAIL treatment (8).

MicroRNAs (miRNAs) are evolutionarily well-conserved, small non-coding transcripts. It plays an important role in the post-transcriptional regulation of target mRNA via mRNA degradation or translational repression through binding with 3′-untranslated regions (UTRs) of target genes. Accumulating evidences demonstrated that miRNAs play a critical role in the regulation of malignant behaviors of cancer cells (9). A systematic study has reported that a series of miRNAs is involved in regulation of TRAIL-induced cell death in the lung cancer cells (10). And the further mechanistic study showed that the growth factor induced upregulation of miR-221 and miR-222 inhibits TRAIL-induced apoptosis by targeting PTEN (11). And more strikingly, recent studies reported that cell-secreted miRNAs are predominantly carried by exosomes and exert in post-transcriptional regulation of gene expression in recipient cells through mRNA silencing (12–14).

In the present study, we screened and identified that miR-7 is a *bona fide* sensitizer for TRAIL-induced apoptosis in GBM and also other types of cancer cells. The mechanistic study showed that miR-7-XIAP axis plays a critical role for TRAIL sensitivity in cancers. We sought to evaluate the combined effect of exosome-transferred miR-7 and MSCs-mediated soluble TRAIL (sTRAIL) delivery on tumor growth *in vitro* and *in vivo*. We confirmed here that combining miR-7 overexpression with sTRAIL leads to synergistic tumor suppression effect *in vitro* and *in vivo*. Our study provides evidence for the co-delivery of sTRAIL and tumor suppressor miRNAs by MSCs to tumor tissues via exosomes and may highlight a novel therapeutic strategy for GBM.

MATERIALS AND METHODS

Cell culture

Human embryonic kidney cell lines (HEK-293A and HEK-293T), human hepatocellular carcinoma (HCC) cell lines (Hep G2 and SMMC-7721) and human GBM cell lines (U-87 MG, U251, A-172, T98G) were obtained from the Shanghai Institutes for Biological Sciences (Chinese Academy of Sciences, Shanghai, China). Adherent cultures of HEK-293A, HEK-293T, Hep G2, U-87 MG, U251, A-172 and T98G cell lines were maintained in Dulbecco's modified Eagle's medium (DMEM)(Life Technology, Grand Island, NY, USA) supplemented with 10% fetal bovine serum (FBS)(Life Technology, Grand Island, NY, USA). The SMMC-7721 cell line was maintained in RPMI-1640 medium (Life Technology, Grand Island, NY, USA) supplemented with 10% FBS. Isolation and expansion of the Mouse Bone Marrow Mesenchymal Stem Cell (BMMSCs) was done based on a published method (15). Then MSCs were maintained in OriCellTM Balb/c Mouse Bone Marrow Mesenchymal Stem Cell Complete Medium (Cyagen, Silicon Valley, CA, USA). All the cells were incubated in a humidified atmosphere of 5% CO_2 in air at 37°C. For the mixed co-culture experiments, tumor cells were mixed with an equal number of MSCs in a 6-well plate and MSCs were processed with different ways 12 h before the cocultivation. Co-culture was maintained for 2 days before flow-cytometry-based separation.

Transfection and lentiviral transduction

Cells were seeded in 6-well plates (2×10^5 cells/well), or 60-mm dishes (5×10^5 cells/dish) or 100-mm dishes (2×10^6 cells/dish), a day before transfection. The transfection was performed when they were at 60–80% confluence. Cells were transfected with miR-7/NC mimics (GenePharma, Shanghai, China), miR-7/NC inhibitor (GenePharma, Shanghai, China), XIAP-siRNA (GenePharma, Shanghai, China) or plasmids, which were listed in Supplementary Table S1. All transfections were performed using Lipofectamine 2000 (Invitrogen, Carlsbad, CA, USA) following the manufacturer's instructions. To minimize toxicity, the transfection complex was replaced with fresh medium 6 h later. Analyses on recipient cells or further research were performed 48 h after transfection.

Packaging of lentivirus was performed using a transient co-transfection system of HEK-293T cells in 60-mm dishes with 1 μg pMD2G, 3 μg psPAX2 and 4 μg pLenti6.3-mcherry/Luciferase/TRAIL/miR-7 and the polymerase chain reaction (PCR) cloning primers for these genes were listed in Supplementary Table S2. Twenty-four hours post-transfection, supernatants were harvested and medium were changed with fresh medium for the second harvest 24 h later. Both the two supernatants were mixed and used to infect target cells. For lentiviral transduction of MSCs, MSCs were plated at a density of 5×10^4 cells per well in 24-well plates and cultured overnight prior to transduction. The medium was replaced with the infection complex medium which is composed of 500 μl lentiviral supernatant (LV-mcherry or LV-Luciferase or LV-TRAIL or LV-miR-7), 500 μl fresh medium and 8 μg polybrene (Sigma, St Louis, MO, USA) to assist the uptake of viral particles. Then the plates were centrifuged with 2100 rpm at 37°C for 1 h followed by replacement of fresh medium. After infection, cells were screened by culturing in the presence of 7 μg/ml blasticidin for 7 days and DsRed fluorescence (mcherry) was observed under a fluorescence microscope (IX71, Olympus, Tokyo, Japan).

RNA isolation and qRT-PCR

Total RNA from cells, tissues and exosomes were isolated using TRIzol Reagent (Invitrogen, Carlsbad, CA, USA) according to manufacturer's instructions. RNA content was measured using a Nanodrop-2000 (Thermo Fisher Scientific, Waltham, MA, USA). One microgram of RNA was employed to synthesize cDNA using the PrimeScript RT Reagent Kit Perfect Real Time (TaKaRa, Dalian, China) or the miScript II RT Kit (Qiagen, Hilden, Germany). To determine the amount of the individual miRNA and mRNA levels, we employed the fluorescent quantitative real time PCR (qRT-PCR) using the Fast SYBR Green Chemistry (TaKaRa, Dalian, China) on Bio-Rad C1000 Thermal Cycler (Bio-Rad, Hercules, CA, USA). All the primers listed

in Supplementary Table S3 were obtained from AuGCT Co. (Beijing, China). The reactions were performed in a 20 μl volume in triplicate with the following amplification steps: an initial denaturation step at 95°C for 3 min, followed by 44 cycles of denaturation at 95°C for 10 s, anneal at 56°C for 15 s and extension at 72°C for 15 s. Finally, the relative quantities of miRNA and mRNA were calculated using $2^{-\Delta\Delta CT}$ method after normalization to RNU6B or GAPDH or miR-16.

MicroRNA microarray, target gene prediction and luciferase reporter assay

Total RNA was extracted from four cancer cell lines. The microRNAs expression pattern was analyzed using Cancer Focus microRNA PCR Panel, 96 well (Exiqon, Vedbaek, Denmark). Target genes of microRNA were determined from the union of miRNA target predictions from TargetScan 6.2 (http://www.targetscan.org) and PicTar (http://pictar.mdc-berlin.de/cgi-bin/PicTar_vertebrate.cgi). The luciferase reporter assay about the regulatory relationship between miR-7 and XIAP was performed using the same method ever before (16).

Western blot and ELISA

Total cell lysates were analyzed by western blotting as previously described (17). The antibodies used were listed in Supplementary Table S4. An enzyme-linked immunosorbent assay (ELISA) was used to detect TRAIL secretion ability using a commercial TRAIL ELISA kit (R&D systems, Minneapolis, MN, USA) according to the manufacturer's instructions.

Flow cytometry analysis

Flow cytometry was used to perform tumor cell isolation from co-culture. Cells were trypsinized and collected after 48 h cocultivation. After centrifugation and resuspension of cell pellet to a single-cell suspension, cells were washed twice in phosphate-buffered saline (PBS) and re-suspended in PBS, stained with phycoerythrin (PE)-conjugated anti-CD44 mouse antibody (BioLegend, San Diego, CA, USA) or PE-conjugated mouse IgG1, κ Isotype ctrl (BioLegend, San Diego, CA, USA) for 30 min at 4°C. After twice washes of PBS, cells were analyzed on a flow cytometer (BD FACSAriaTM Cell Sorter, BD Biosciences, San Jose, CA, USA). The CD44 negative tumor cells were isolated and used to make further research, such as qRT-PCR, western blot and apoptosis studies.

Cells were analyzed for their surface markers or molecular receptors using flow cytometry. MSCs were stained with PE-conjugated anti-CD44 mouse antibody (BioLegend, San Diego, CA, USA), FITC-conjugated anti-CD90 mouse antibody (BioLegend), Percp-conjugated anti-CD45 mouse antibody (BioLegend), FITC-conjugated anti-Sca-1 mouse antibody (BioLegend). GBM cells were stained with PE-conjugated anti-DR4 mouse antibody (BioLegend) and PE-conjugated anti-DR5 mouse antibody (BioLegend) or PE-conjugated mouse IgG1, κ Isotype ctrl (BioLegend) and analyzed on a flow cytometer (Epics XL.MCL, BECKMAN COULTER, Brea, CA, USA).

Apoptosis studies

Cells were collected and suspended in PBS after 48 h TRAIL (300 ng/ml) (Peprotech, Rocky Hill, NJ, USA) treatment. The CD44 negative tumor cells were isolated after 48 h cocultivation and suspended in PBS. The obtained cells were stained with Annexin-V-FLUOS Staining kit (Roche, Mannheim, Germany) and analyzed on a flow cytometer (Epics XL.MCL, BECKMAN COULTER, Brea, CA, USA). Cell apoptosis in xenograft tumor samples was detected by TUNEL staining using an In Situ Cell Death Detection Kit, Fluorescein (Roche, Mannheim, Germany) according to the manufacturer's protocol. The nuclei were then counterstained with 1.5 μg/ml 4, 6-diamidino-2-phenylindole dihydrochloride(DAPI) (Sigma-Aldrich, St Louis, USA) at room temperature for 3 min. After being washed in PBS, samples were subjected to laser scanning confocal microscopy analysis (A1, Nikon, Tokyo, Japan).

Live cell imaging system

U-87 MG cells were transfected with pCDNA3.1-GFP, and MSCs were transfected with miR-7-Cy3 (GenePharma, Shanghai, China). They were collected and mixed as a ratio of 1:1 12 h after transfection, then seeded in 96-well plate (100 cells/well). They co-cultured for 24 h, and were submitted to Live cell imaging system (A1, Nikon, Tokyo, Japan). The fluoresence location of cells was monitored for 48 h, and the images were captured once every 15 min during this time. Finally, the images were used to form a video, which could verify the communication type of cells according to the changes of fluoresence location.

In vitro cell differentiation

MSCs were plated in 6-well plate (1×10^5 cells/well), and supplemented with appropriate differentiation medium for the induction of MSCs differentiation into different phenotypes. MSCs were cultured using OriCell™ Balb/c Mouse Bone Marrow Mesenchymal Stem Cell Osteogenic Differentiation Medium Kit (Cyagen, Silicon Valley, CA, USA) and Adipogenic Differentiation Medium Kit (Cyagen, Silicon Valley, CA, USA) for 4 weeks, and staining was performed to confirm osteogenic and adipogenic differentiation ability according to the manufacturer's instructions provided by the kit. Then the images were captured using a microscope (CK40, Olympus, Tokyo, Japan).

In vitro migration assay

The ability of MSCs to migrate to cancer cell lines was measured in 24-well plates using Corning transwell chambers with 8 μm filter membranes (Corning, Acton, MA, USA). HEK-293A cell line was used as a negative control. U-87 MG, U251 and HEK-293A cells were incubated in serum-free medium for 48 h, and the resulting conditioned media (CM) was used as a chemoattractant. Either MSCs or MSCs-Luc/TRAIL (2×10^4 cells) were resuspended in 300 μl of serum-free α-minimum essential medium containing 0.1% bovine serum albumin and loaded in the upper compartment. The lower compartment was filled with 600 μl of the CM. After incubation at 37°C in 5% CO_2 for 6 h, the

non-migrated cells were removed from the upper surface of the membrane using cotton swabs. Cells that had migrated to the lower surface were fixed with 4% paraformaldehyde and stained with crystal violet. The number of cells that had migrated to the lower side of the filter was counted under a microscope (CK40, Olympus, Tokyo, Japan) with five random fields (magnification, × 4).

Xenograft tumor model

Male athymic Balb/c nude mice (4–6 weeks, 20–25 g) were purchased from the Experimental Animal Center, Chinese Academy of Science (Shanghai, China). All animal experiments were approved by the Animal Experiment Administration Commission of Fourth Military Medical University (FMMU). Approximately 1×10^7 U-87 MG cells in 200 μl PBS were injected subcutaneously into the left flank of each mouse. Tumor volume was monitored using a caliper once every three days. Once the tumors reached 100 mm^3 as calculated by ($\pi \times$ length $\times$ width^2)/6, they were divided into six groups randomly, six mice per group. MSCs stable cell lines were transiently transfected with miR-NC or miR-7. Then modified MSCs were injected into the Balb/c nude mice via tail vein once every three days (5×10^5 cells/mouse), meanwhile the tumor volume was measured. Mice were killed by spinal dislocation when they were treated seven times. Then tumors were removed and weighed, after that, tumors and organs (such as the heart, liver, spleen, lungs, kidneys and brain) were snap-frozen in liquid nitrogen for further research or fixed in formalin for immunohistochemical (IHC) analysis, morphological analysis and apoptosis analysis.

In vivo homing assay

MSCs homing to the tumor sites *in vivo* were determined by IHC. Subcutaneous xenograft tumor models were generated by inoculation of 1×10^7 U-87 MG cells into Balb/c nude mice as described above. When tumors reached 100 mm^3 as calculated by ($\pi \times$ length $\times$ width^2)/6, 5×10^5 miR-7 loaded TRAIL-MSCs were injected via tail vein and the primary tumor was harvested after 16 h injection. The TRAIL expression level was determined by IHC assay using the anti-TRAIL antibody (Cell Signaling Technology, Danvers, MA, USA).

Exosome isolation and inhibition of exosome secretion

Cells were cultured for 48 h and exosomes were collected from their culture media after sequential ultracentrifugation as described previously (18). Briefly, cell culture media were collected, centrifuged at 300 *g* for 5 min, 1500 *g* for 10 min and then further centrifuged 12 000 *g* for 35 min. Then supernatants were filtered through a 0.22 μm filter (Merck Millipore, Tullagreen, Ireland), followed by ultracentrifugation at 120 000 *g* for 2 h to pellet the exosomes. The exosome pellets were washed once with 20 ml cold PBS and further purified by centrifugation at 120 000 *g* for 2 h. The temperature was at 4°C in the whole centrifugation process. The final pellet containing exosomes was resuspended in 50–100 μl PBS and stored at −80°C until be used for (i) adding into the cell culture media; (ii) transmission electron microscopy; and (iii) qRT–PCR.

Exosome release was blocked by specific inhibitors GW4869 (Sigma, St Louis, MO, USA) and DMA (Santa Cruz, Paso Robles, CA, USA). To validate that miRNAs and mRNAs were transferred via exosome, cells were treated with GW4869/DMA/DMSO, DMSO was used as negative control. MSCs were transfected with miRNA mimics in 6-well plates. For exosome isolation, the cells were cultured for 48 h, the culture medium was collected and used for exosome preparation. The exosomes were added to U-87 MG mono-culture for 48 h. For cocultivation, the cells were reseeded and co-cultured with tumor cells in 6-well plates for 48 h with 10 μM GW4869 or 15 nM DMA, or DMSO. Then the cells were used for (i) fluorescence microscopy; (ii) isolation of tumor cells; and (iii) qRT–PCR.

Transmission electron microscopy

For electron microscopy analysis, exosomes were prepared in PBS. The samples were adsorbed to carbon-coated nickel grids and negatively stained for 5 min with 2% methylamine tungstate. Then stain was blotted dry from the grids with filter paper and washed twice on drops of distilled water. Afterward the water was blotted dry and samples were allowed to dry. Samples were then examined in a JEM-1230 electron microscope (Nihon Denshi, Tokyo, Japan) at an accelerating voltage of 80 kV.

Hematoxylin and Eosin (HE) Staining

The toxicity of modified MSCs was tested in male Balb/c mice (6-weeks-old). HE staining of major organs was carried out for histological observation as previously described (19). Images were taken by light microscope (BX51, Olympus, Tokyo, Japan).

Immunohistochemistry

Standard IHC staining was performed as previously described (20). In brief, after de-paraffinization and rehydration, sections were subjected to heat-induced antigen unmasking. Slides were then incubated with various primary antibodies at 4°C overnight, after blocking with 5% goat serum. Slides underwent color development with DAB (BD Pharmingen, New York, NJ, USA) and haematoxylin (Vector Laboratories, Burlingame, CA, USA) counterstaining. Images were captured with a microscope (BX51, Olympus, Tokyo, Japan) and processed with identical settings. Ten visual fields from different areas of each tumor were evaluated.

Patient samples

Twenty GBM tissues were obtained from the department of Neurosurgery in Xijing Hospital, which is a subsidiary hospital of the Fourth Military Medical University (FMMU). Collection of tumor samples was approved by the Moral and Ethical Committee of FMMU. The 20 frozen tumor samples (∼0.2 mg each) were used for RNA isolation, and then were used to analyze the correlation between miR-7 and XIAP expression level using qRT-PCR assay.

Statistical analyses

Statistical analyses were performed using GraphPad Prism version 5.00 (GraphPad Inc., La Jolla, CA, USA). Data are expressed as the means ± SD from at least three separate experiments. Experiments with two experimental groups were evaluated using Two-tailed Student's *t*-test. In experiments with more than two experimental groups, one-way ANOVA with Tukey's post-test was used. The significance of associations between gene expression values was judged via a test statistic based on Pearson product-moment correlation coefficient. The results were considered statistically significant when $*P < 0.05$; $**P < 0.01$; $***P < 0.001$.

RESULTS

Global analysis of microRNAs positively associated with TRAIL sensitivity in GBM cells

We analyzed TRAIL sensitivity of different human GBM cell lines: U-87 MG(U87), U251, A-172(A172) and T98G. Cells were exposed to TRAIL and cell death was assessed using fluorescence-activated cell sorting (FACS) with Annexin-V and propidium iodide(PI) staining. As shown in Figure 1A, T98G cells underwent TRAIL-induced cell death whereas U87 and U251 cells did not display sensitivity when exposed to TRAIL, A172 cells showed an intermediate sensitivity. A possible mechanism of the differential sensitivity of the tested cells to TRAIL induced apoptosis could be due to the variability of the cell surface levels of the death receptors. However, the result of the expression levels of TRAIL receptor DR4 and DR5 revealed comparable expression levels of them in TRAIL-sensitive compared to TRAIL-resistant cells (Supplementary Figure S1). Therefore, it can rule out the possibility of the different expression levels of DRs as a major reason for different sensitivity for TRAIL-induced apoptosis in GBM cells.

To investigate the involvement of miRs for TRAIL sensitivity in GBM cells, we analyzed the miRs expression profile in TRAIL-sensitive cell line (T98G) and semi-resistant cell line (A172) and TRAIL-resistant cell lines (U87 and U251). The analysis was performed with a cancer focus miRNA PCR panel. As shown in Figure 1B, the expression patterns of a serial of miRNAs (such as miR-7, let-7f/g, miR-15b, miR-101) were positively associated with the sensitivity of GBM cells to TRAIL-induced apoptosis. Among them, the miR-7 expression level had the most closely linear relationship with the sensitivity of TRAIL-induced cell death (Figure 1C).

miR-7 is a natural sensitizer for TRAIL-induced apoptosis in glioblastoma cells

To determine the functional association between miR-7 and TRAIL sensitivity in GBM cell lines, we transiently transfected U87 and U251 cells with miR-7 mimics and negative control. Increased expression of miR-7 upon transfection was confirmed by quantitative real time PCR (qRT-PCR) (Figure 2A). Twenty-four hours after transfection, cells were exposed to TRAIL for 48 h and then assessed by Annexin-V staining. Apoptosis assays demonstrated that enforced miR-7 expression raised the proportion of apoptotic cells evidently with regard to their respective controls (Figure 2B). The pro-apoptotic effect of miR-7 combined with TRAIL incubation was further confirmed by Western blot analysis for cleaved caspase-3 (Figure 2C). Conversely, knockdown of miR-7 by anti-miR oligonucleotides (Figure 2D) in A172 and T98G cells induced a decreased apoptotic rate (Figure 2E). The data indicate that miR-7 facilitates sensitivity to TRAIL-induced apoptosis in GBM cells.

Furthermore, we wondered to know that if pro-apoptotic effect of miR-7 combined with TRAIL is a cancer type specific molecular event or a general characteristic. MiR-7 mimics were transiently transfected into two HCC cell lines (Hep G2 and SMMC-7721) (Figure 2A). Similar results were obtained in these two cell lines (Figure 2B and C), suggesting that miR-7 is definitely involved in regulating sensitivity to TRAIL-induced cell death in multiple types of tumor cells.

XIAP is a direct target of miR-7 in multiple types of tumor cells

To identify miR-7-mediated downstream regulators for TRAIL sensitivity in GBM cells, two target prediction algorithms (PicTar (21) and Targetscan (22)) were applied (Figure 3A). The 1188 picks from the algorithms were further analyzed according to the PANTHER classification system (23), in which 26 genes were clustered in the apoptotic process (Figure 3B). Using qRT-PCR, we found that the mRNA levels of three genes including XIAP, BCL2L1 and SMOX were downregulated significantly (Figure 3C). Among them, SMOX is a spermine oxidase. Although it was reported as a pro-apoptotic molecule, its function is closely associated with oxidative stress-induced DNA damage and apoptosis (24). Oxidase stress is not a major causation in TRAIL-induced apoptosis. According to this evidence, we did not further investigate the contribution of SMOX for miR-7 in TRAIL-induced apoptosis. I also ruled out BCL2L1 as a candidate is because that TRAIL induces the extrinsic apoptosis pathway, while BCL2L1 is involved in the intrinsic apoptosis pathway (25). Then we considered XIAP (Figure 3C), a known regulator of anti-apoptosis, as an excellent candidate (26,27). And it occurs coincidently that XIAP was reported to be involved in miR-7 induced inhibitory proliferation of cervical cancer cells (28). Overexpression of miR-7 in TRAIL-resistant GBM cells resulted in a significant decrease of XIAP in both mRNA (Figure 3D) and protein (Figure 3E) levels. Whereas, knockdown of the endogenous miR-7 by the antagonist increased XIAP protein levels in TRAIL-sensitive GBM cells (Figure 3F). Strikingly, the XIAP inhibition by miR-7 was also observed in other types of cancer cell lines (Figure 3D and E). Analysis using 3′ untranslated region (UTR) luciferase reporter plasmids containing the miR-7 target sequences (wild-type or mutant) on XIAP was performed to determine whether XIAP is a direct target of miR-7. Expression of miR-7 caused a significant decrease in luciferase activity in the wild-type XIAP 3′ UTR, but not in the mutant form (Figure 3G). Taken together, these results indicate that XIAP is a *bona fide* target of miR-7 in multiple types of tumor cells.

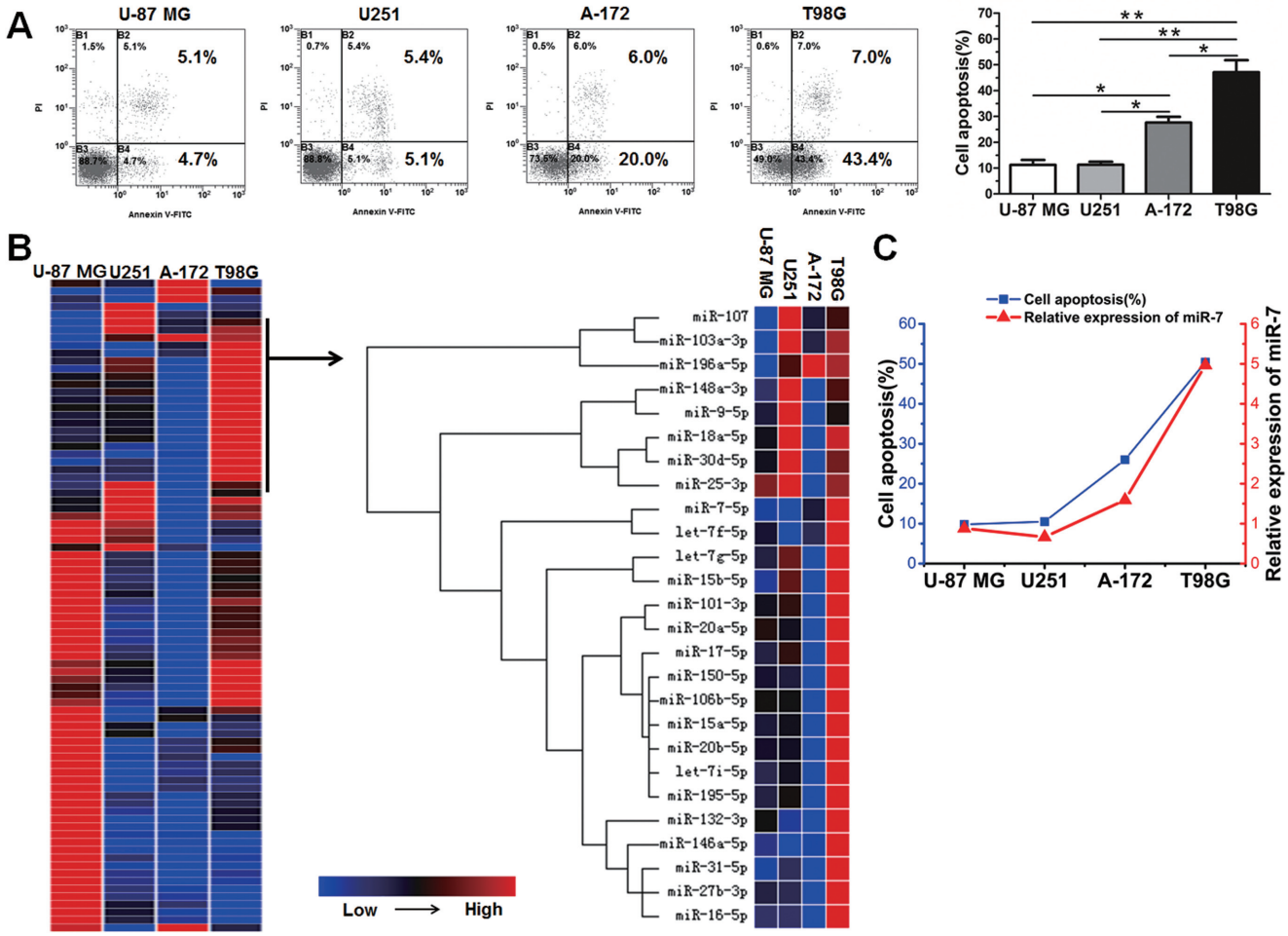

Figure 1. High-throughput functional screening for miRNAs which modulate glioblastoma TRAIL-sensitivity. (**A**) Cell apoptosis of GBM cells after 48 h TRAIL treatment determined by FACS analysis with Annexin-V and PI staining (mean ± SD, $n = 3$). (**B**) Candidate TRAIL sensitizing miRNA verification by a cancer focus miRNA PCR panel. The miRNAs were organized based on the expression profiling. (**C**) The correlation between miR-7 expression and TRAIL-induced apoptosis. The expression level of miR-7 in GBM cells was confirmed by qRT-PCR analysis. $^{*}P < 0.05$, $^{**}P < 0.01$.

The miR-7-XIAP axis is crucial for TRAIL sensitivity in cancer cells

To determine the contribution of the miR-7-XIAP axis for TRAIL induced apoptosis in cancer cells, we silenced the endogenous expression of XIAP in multiple GBM and HCC cells as shown in Figure 4A and Supplementary Figure S2A. The result of Annexin-V staining showed that knockdown of XIAP significantly increases apoptotic ration of cancer cells treated with TRAIL (Figure 4B), but does not increase apoptosis without TRAIL treatment (Supplementary Figure S2B). Conversely, when we reintroduced exogenous XIAP without 3′ UTR into miR-7 expressing tumor cells, the expression levels of XIAP and miR-7 were confirmed as shown in Figure 4C and Supplementary Figure S2C and D. Overexpression of XIAP attenuates miR-7-mediated TRAIL sensitivity in GBM cells (Figure 4D). As expected, similar phenotypes were also observed in HCC cells (Figure 4D). Rescue experiment demonstrates the causative link between the miR-7-XIAP axis and TRAIL sensitivity in cancer cells.

Then we asked that if the miR-7-XIAP axis does exist in tumor cell lines and clinical tumor tissues. We performed qRT-PCR assay to measure the endogenous expression levels of miR-7 and XIAP in cancer cell lines. First, we observed a dramatically inverse correlation between miR-7 and XIAP in GBM cell lines (Figure 4E). Then we found the similar relationship in HCC cells (Hep G2, SMMC-7721, HuH-7 and MHCC-97H) and prostate cancer cells (PC-3, PC-3M, DU 145, 22Rv1 and LNCaP) (Figure 4F). To further confirm whether this correlation also exists in human tumor tissues, we analyzed 20 tumor samples from GBM patients using qRT-PCR, and found that the expression of XIAP was reversely associated with the expression of miR-7 (Figure 4G). The data indicate that XIAP is crucial for mir-7-mediated TRAIL sensitivity in cancer cell lines and the inverse relationship between miR-7 and XIAP exists in multiple types of tumor cell lines and clinical patient samples.

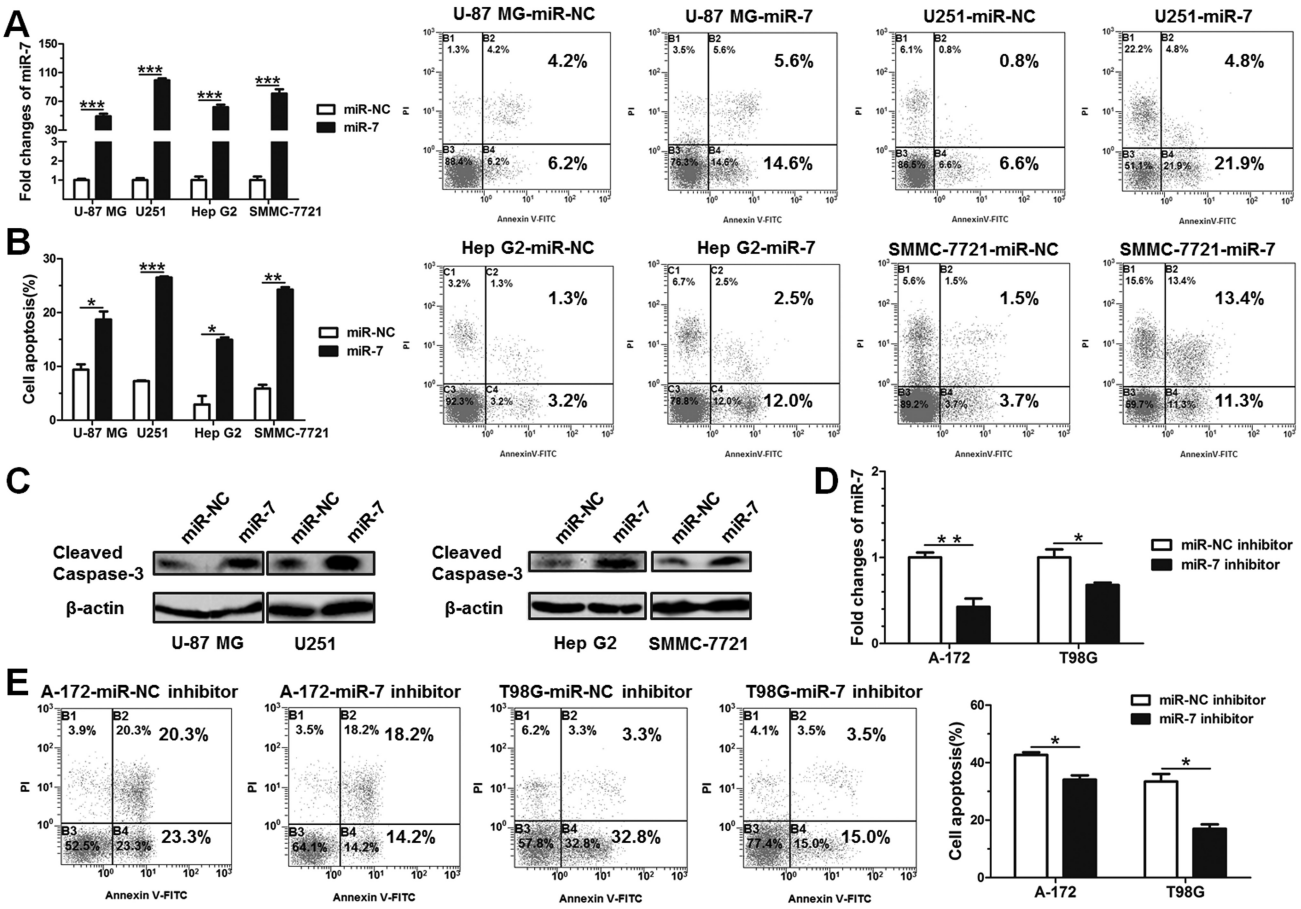

Figure 2. MiR-7 overexpression enhances TRAIL sensitivity in human GBM and HCC cell lines. (**A**) qRT-PCR analysis confirming the changes of miR-7 in cells transfected with control or miR-7 and normalized to RNU6B expression. (**B**) Percent cell apoptosis of four cancer cell lines initially transfected with control or miR-7 24 h followed by 48 h treatment of TRAIL determined by Annexin-V assay. (**C**) Western blot analysis determining the change of cleaved caspase-3 in control or miR-7-treated cancer cells. β-actin was used as control. (**D**) qRT-PCR analysis showing changes in the relative miR-7 expression represented graphically in control, miR-7 inhibitor treated sets. (**E**) Percent cell apoptosis of cancer cells for the aforementioned sets. Results are presented as mean ± SD by *t*-test. ($n = 3$) $^{*}P < 0.05$, $^{**}P < 0.01$, $^{***}P < 0.001$.

miR-7-enriched exosomes are efficiently released from TRAIL expressing MSCs and enhance TRAIL sensitivity *in-vitro*

Utilization of MSCs as cellular vehicles has been demonstrated to be a promising approach to deliver TRAIL to cancer tissues (8). However, TRAIL-expressing MSCs (TRAIL-MSCs) do not tackle the intrinsic resistance of cancer cells toward TRAIL. We hypothesized that exogenous miR-7 may be transferred from TRAIL-MSCs to cancer cells in an exosome-dependent manner. In this process, the miR-7-XIAP axis could counteract TRAIL resistance of cancer cells in TRAIL-MSCs recruited local tissues.

We used lentiviral expression system to overexpress sTRAIL in MSCs. And Firefly Luciferase or mCherry expressing MSCs (Luc-MSCs, mCherry-MSCs) were also prepared as control groups. As shown in Figure 5A, our viral delivery system efficiently expressed sTRAIL or other control proteins (mCherry) in MSCs. Western blot analysis showed high levels of sTRAIL expression in TRAIL-MSCs cells. And ELISA assay further confirmed the secretory form of sTRAIL in supernatants of genetically modified MSCs (Figure 5B). Meanwhile, we transiently transfected miR-7 mimics into genetically modified MSCs. Apoptotic assay showed that overexpression of miR-7 did not induce obvious cell death in MSCs (Supplementary Figure S3A). Also, cell differentiation ability was not affected by TRAIL and/or miR-7 overexpression (Supplementary Figure S3B). We used qRT-PCR to measure expression levels of miR-7 in MSCs and MSCs-derived exosomes. The result showed that compared with it in miR-NC group cells, significantly higher levels of miR-7 can be tested in miR-7-transfected MSC cells and cell-derived exosomes (Figure 5C). These results indicate that miR-7-enriched exosomes are efficiently released from TRAIL expressing MSCs.

To confirm that miR-7 could be transferred to cancer cells via exosomes from MSCs, we transfected MSC cells with Cy3-labeled miR-7 mimics and exosomes were isolated (Figure 5D). As shown in Figure 5E, after incubation with exosomes, the Cy3 fluorescence signal was observed in most U87 cells. Furthermore, in a co-culture assay, MSCs with transfected Cy3-labeled miR-7 mimics were co-cultured with U87 cells. The result of confocal fluorescence analysis showed that miRNAs could transfer from donor

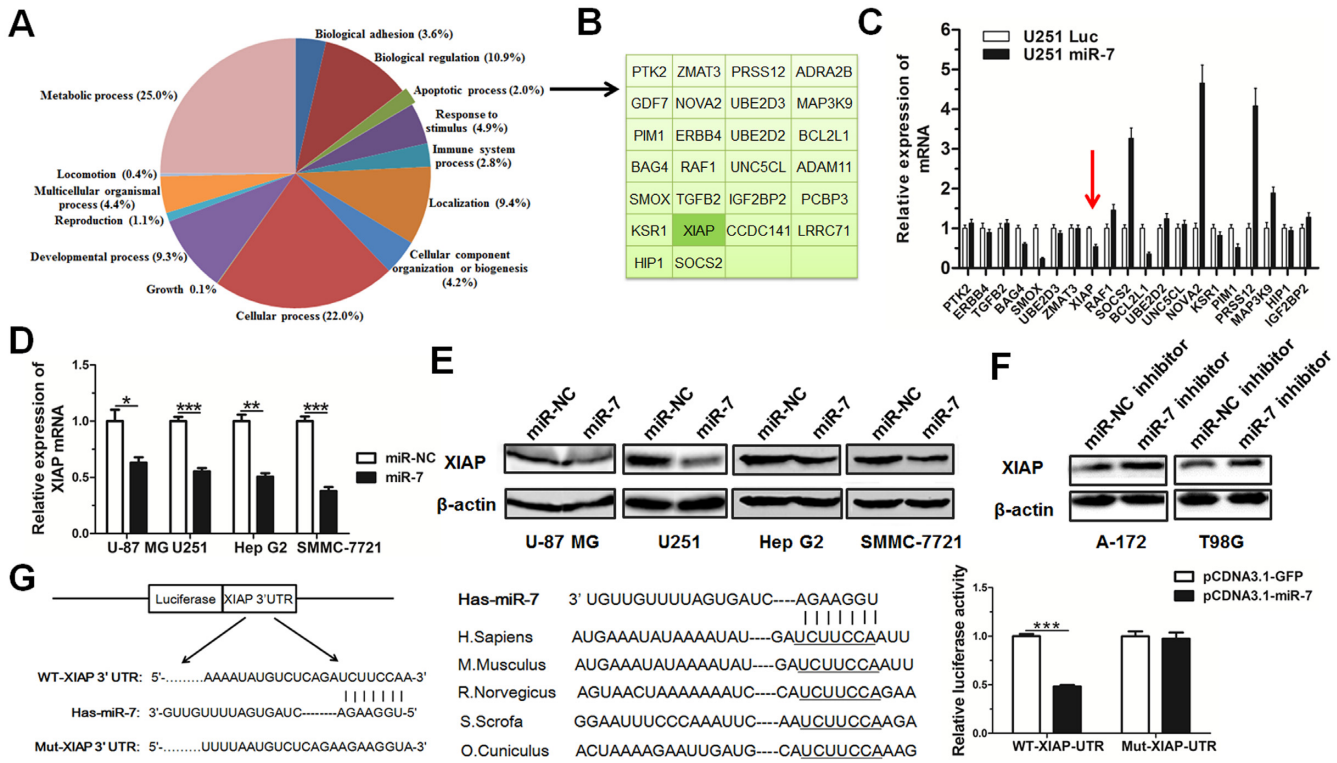

Figure 3. XIAP is a direct target of miR-7 in cancer cells. (**A**) Predicted target genes of miR-7 analyzed according to the PANTHER classification system. These genes were collected from two target prediction algorithms (PicTar and Targetscan). (**B**) Gene list correlated with the apoptotic process. (**C**) qRT-PCR analysis depicting the changes in the expression pattern of these genes in control and miR-7-treated cancer cells and normalized to GAPDH expression. (**D**) qRT-PCR assays (mean ± SD, $n = 3$) of four cancer cell lines 48 h after control or miR-7 mimetic transfection. (**E**) Western blot assays of cancer cells after the transfection. β-actin was used as internal loading control. (**F**) Western blot analysis determining the changes in XIAP expression level for control, miR-7 inhibitor-treated sets. (**G**) Predicted binding site of miR-7 to the XIAP 3′UTR (left panel); Highly conserved binding site across different species (middle panel); Renilla luciferase activity analyses (mean ± SD, $n = 3$) in HEK-293A cells co-transfected with Luciferase-XIAP 3′UTR fusion and miR-7 or vector, 48 h post-transfection (right panel). $^*P < 0.05$, $^{**}P < 0.01$, $^{***}P < 0.001$.

cells to receipt cells (Figure 5F). The transfer process was recorded in Supplementary Video. The cell surface marker expression level of MSCs and U87 cells were analyzed by FACS (Supplementary Figure S4A), and the data indicate that CD44 marker could be used to distinguish the two cell types (Supplementary Figure S4B). To determine the role of exosomes in this miRNA-transferring process, we reduced exosome production using GW4869 (an inhibitor of neutral sphingomyelinase-2) (29) and DMA (an inhibitor of the $H^+/Na^+$and Na^+/Ca^{2+}exchangers) (30). As shown in Figure 5G, the GW4869 and DMA treatment significantly inhibited miR-7 expression levels in U87 cells in the co-culture assay, indicating a critical role of exosomes for the transfer of miR-7 from MSCs to GBM cells. The data demonstrate that the transfer of exogenous miR-7 from MSCs to cancer cells is dependent on exosomes.

To identify whether the exosome-transferred miR-7 can efficiently inhibit endogenous XIAP in cancer cells, we used qRT-PCR to test mRNA levels of XIAP in GBM cells co-cultured with miR-7-loaded MSCs. The result showed that exosome-transferred miR-7 effectively inhibits XIAP expression levels in U87 cells and this effect is significantly blocked by GW4869 and DMA (Figure 5H). Furthermore, we utilized the functional experiment to determine the cancer killing effect of TRAIL and miR-7-armed MSCs *in vitro*. As shown in Figure 5I, overexpression of miR-7 in TRAIL-MSCs significantly induces apoptosis in U87 cells compared with it in control groups. Taken together, TRAIL and miR-7 co-expressing MSCs exert a potential pro-apoptotic effect in an exosome-dependent manner.

miR-7-loaded TRAIL-MSCs specifically migrate to cancer cells (tissues) *invitro* and *invivo*

Tumor tropism is one of the most important reasons for MSCs as a promising delivery vehicle (31). To test whether miR-7-loaded TRAIL-MSCs can specifically migrate to cancer cells *in vitro*, a transwell assay was performed. As shown in Figure 6A, a large number of MSCs migrate to the bottom of Boyden chamber co-cultured with GBM cells compared with an immortalized normal cell line HEK-293A, and the migratory ability of MSCs was not affected by TRAIL and/or miR-7 overexpression. Next, to confirm tumor tropism of MSCs *in vivo*, we established xenograft model of U87 cells in Balb/c nude mice. Genetically modified MSCs were administrated into tumor-bearing mice through tail vein injection. The primary tumor tissues were harvested after 16 h. As shown in Figure 6B, TRAIL and miR-7 co-expressing MSCs were observed expressed in tumor tissues. Taken together, the data indicate that TRAIL

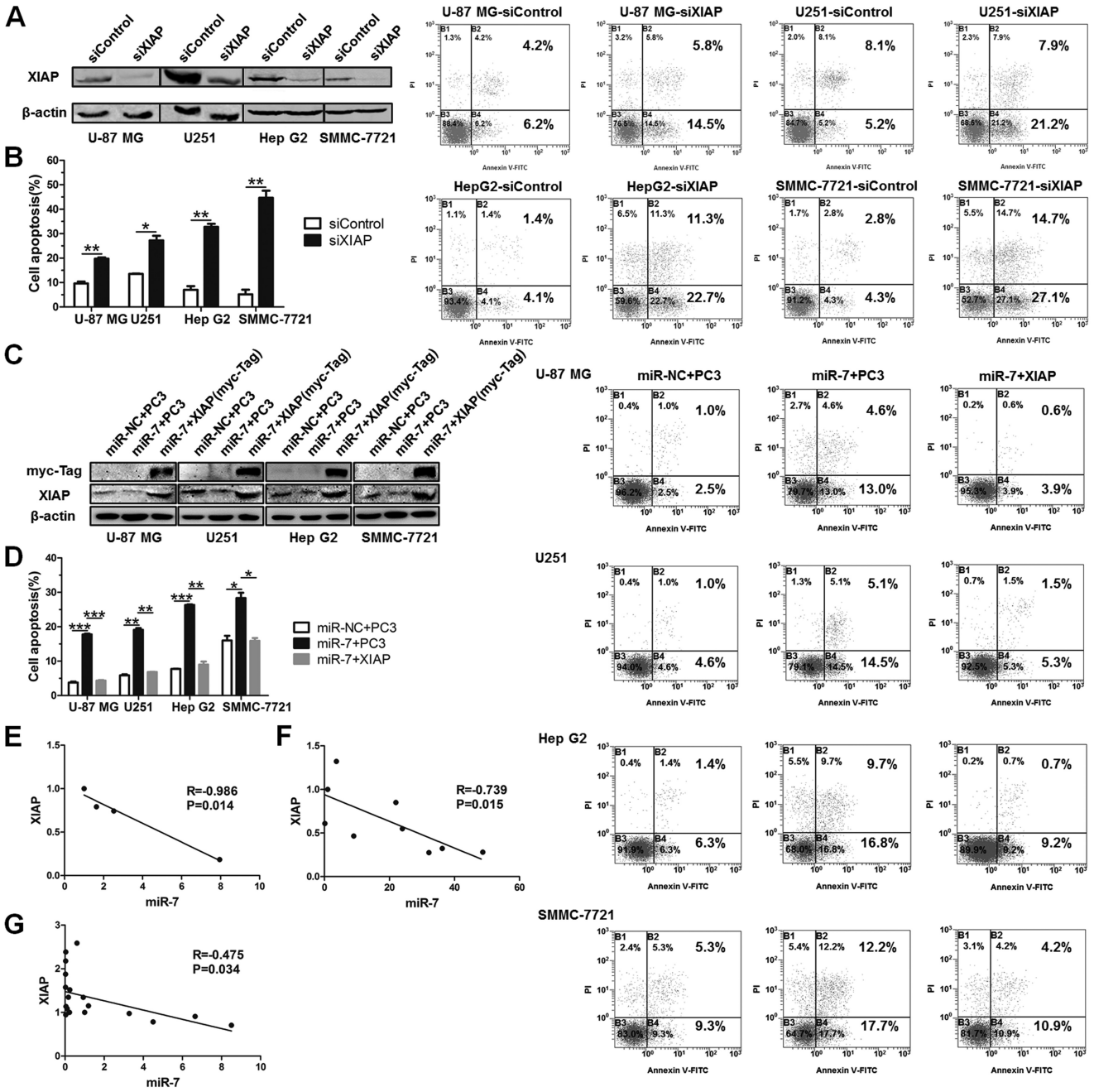

Figure 4. Further validation of miR-7-XIAP axis. (**A**) XIAP knock-down by siRNA (siXIAP) in four cancer cell lines. Western blot assays 48 h after transfection. β-actin was utilized as a loading reference. (**B**) Percent cell apoptosis of cancer cells for the aforementioned sets determined by FACS assay after 48 h treatment of TRAIL.*t*-test, mean ± SD, $n = 3$. (**C**) Western blot analysis determining the changes of XIAP expression level in control, miR-7 with/without XIAP-treated sets. (**D**) Percent cell apoptosis of cancer cells for the aforementioned sets. One-way ANOVA, mean ± SD, $n = 3$. (**E**) The relationship between miR-7 and XIAP in GBM cell lines (U87, U251, A172, T98G) was evaluated using qRT-PCR assay. (**F**) The relationship in four hepatocellular carcinoma cell lines (Hep G2, SMMC-7721, HuH-7 and MHCC-97H) and five prostatic carcinoma cell lines (PC-3, PC-3M, DU 145, 22Rv1 and LNCaP). (**G**) The relationship in GBM clinical samples. $^*P < 0.05$, $^{**}P < 0.01$.

and miR-7 co-expressing MSCs have the characteristic of tumor tropism *in vitro* and *in vivo*.

Therapeutic potential of combined therapy with TRAIL and miR-7 expressing MSCs *invivo*

To evaluate therapeutic benefit of combined expression of TRAIL and miR-7 in MSCs *in vivo*, we used U87 cells to establish tumor xenografts in nude mice. We loaded TRAIL-MSCs either with miR-7 mimics or miR-NC control. When the tumors were palpable, we intravenously injected 5×10^5 modified MSCs into tumor-burdened animals and followed tumor growth over the next 3 weeks. As shown in Figure 7A, although the TRAIL-MSCs treated group exhibits inhibition of tumor growth compared with PBS or only Luc-

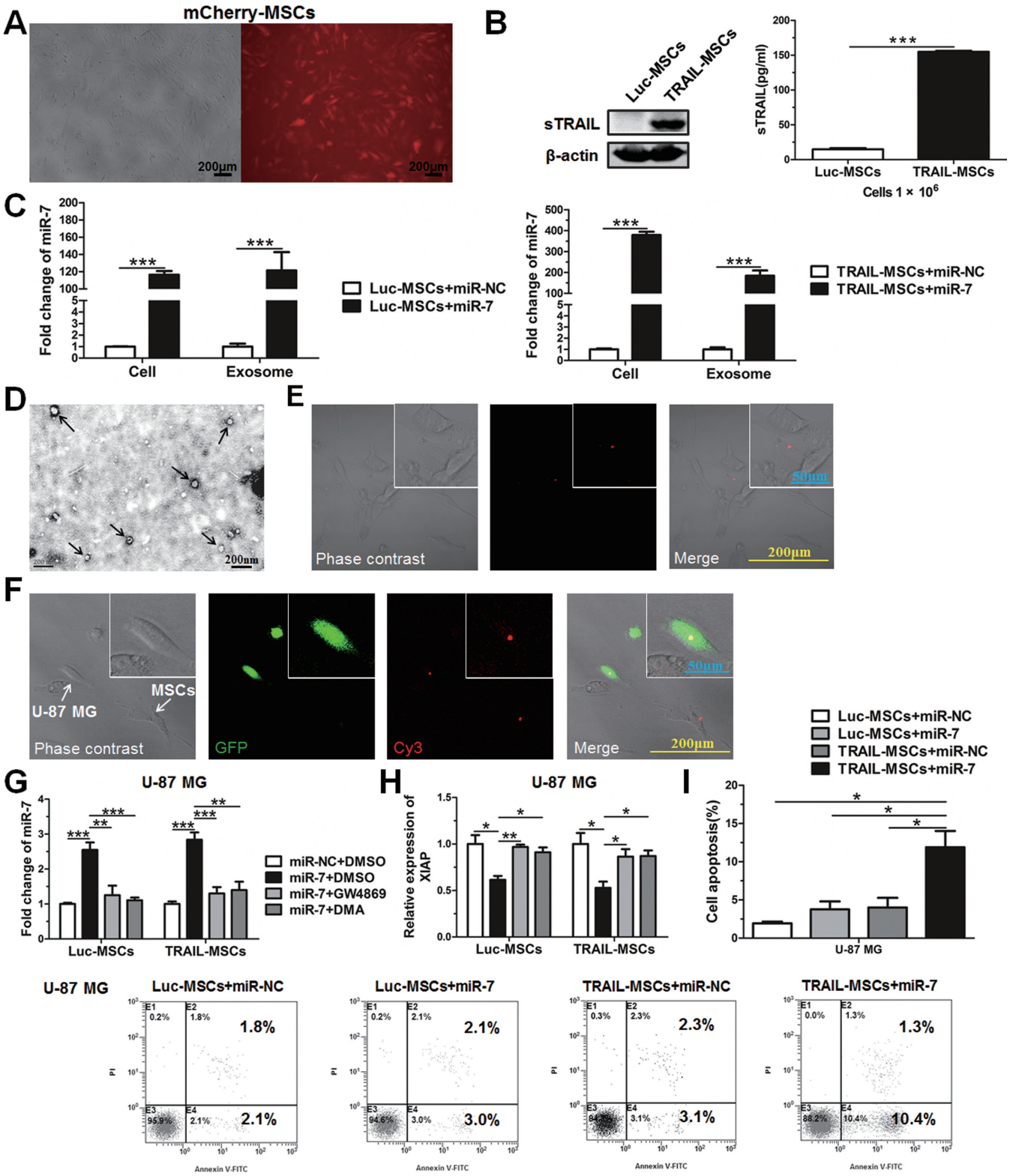

Figure 5. MiR-7-enriched exosomes are efficiently released from TRAIL expressing MSCs and enhance TRAIL sensitivity *in vitro*. (**A**) High transduction efficiency in MSCs by lentivirus-mediated expression of mCherry under the fluorescence microscope. (**B**) Western blot analysis determining sTRAIL expression level in cell lysates (left panel); ELISA assay of sTRAIL in cell supernatants (right panel). (**C**) qRT-PCR analysis of the changes in miR-7 expression level from control, miR-7-treated MSCs and exosomes isolated from the sets. ***$P < 0.001$ by *t*-test. (**D**) Identification of exosomes by transmission electron microscopy. (**E**) Representative data showing presence of Cy3-miR-7 in U87 cells after adding exosomes purified from Cy3-miR-7-transfected MSCs-TRAIL for 48 h. (**F**) Confirmation of the transmissible ability of miR-7 from MSCs to U87 cells by laser scanning confocal microscopy 48 h after the cocultivation of GFP-expressing U87 and miR-7-Cy3 transfected MSCs. (**G**) qRT-PCR analysis determining the changes of miR-7 expression level in U87 cells after the cocultivation. (**H**) qRT-PCR analysis depicting the changes of XIAP expression level. (**I**) Percent cell apoptosis of U87 cells 48 h after the cocultivation. *$P < 0.05$ by one-way ANOVA; mean ± SD, $n = 3$.

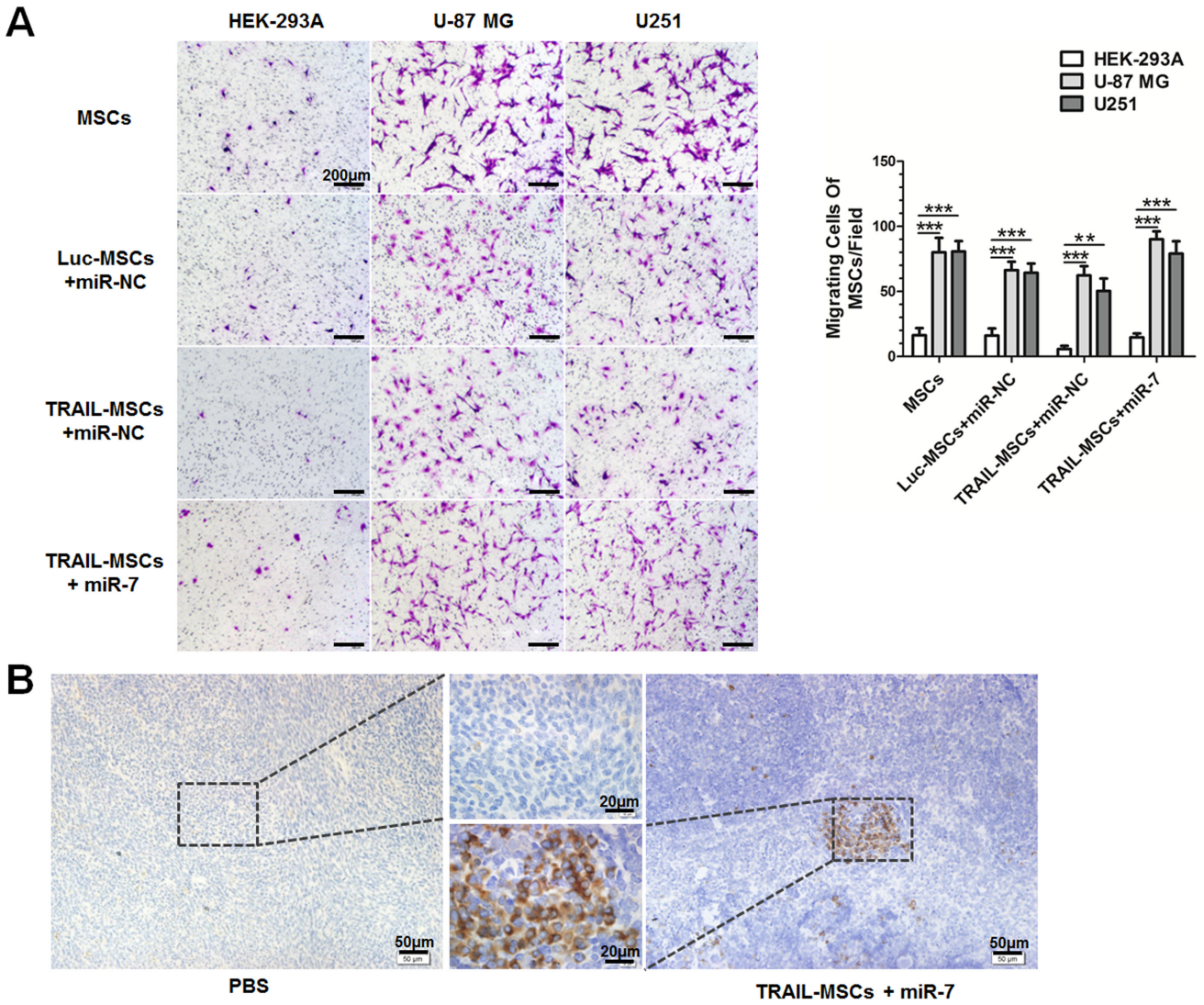

Figure 6. MiR-7-loaded TRAIL-MSCs specifically migrate to cancer cells. (**A**) The migration ability of MSCs with different modification toward cancer cell lines at 6 h as determined from transwell assay *in vitro*. HEK-293A cell was used as a control to better mimic the normal cell lines. Representative photomicrographs of stained filters showing migrated MSCs or modified MSCs. (**B**) Immunohistochemical (IHC) analysis of tumor tissues showing the migration ability of miR-7-loaded TRAIL-MSCs *in vivo*. Tumor tissues were harvested 16 h after tail vein injection using modified MSCs. $^{**}P < 0.01$, $^{***}P < 0.001$; one-way ANOVA, mean ± SD, $n = 3$.

MSCs treated groups, TRAIL/miR-7 co-expressing MSCs have a much stronger impact on growth retardation compared with TRAIL/miR-NC co-expressing MSCs treated groups. In addition, our records for the final tumor weight clearly illustrate the fact that the combinational expression of TRAIL and miR-7 in MSCs leads to tumor regression compared with other tested groups (Figure 7B). Furthermore, analysis of IHC staining showed that compared with other indicated groups, the expression levels of XIAP markedly decreased in tumor tissues treated with miR-7 transfected-MSCs (Figure 7C). This result further validates our discovery that miR-7 could transfer to cancer cells from MSCs and consequently reduce the expression level of XIAP in tumor tissues. And quantifying the number of apoptotic cancer cells in relation to tumor sizes showed that TRAIL and miR-7 co-overexpressing MSCs have a significantly higher effect on cell death compared with other groups (Figure 7D). Moreover, we also evaluated potential toxic side effects of the modified MSCs treatments by histological analysis of organ tissues (heart, liver, spleen, lung and kidney). All tissues appeared normal and no signs of toxicity or apoptosis could be detected (Supplementary Figure S5).

DISCUSSION

Apoptosis-based cancer therapeutics is developed to achieve tumor eradication through the utilization of death inducing molecules capable of activating the apoptotic program selectively in transformed cells. Defects in the apoptotic program may contribute to treatment resistance and tumor progression and may be caused by deregulated expression of anti-apoptotic molecules. TRAIL has the

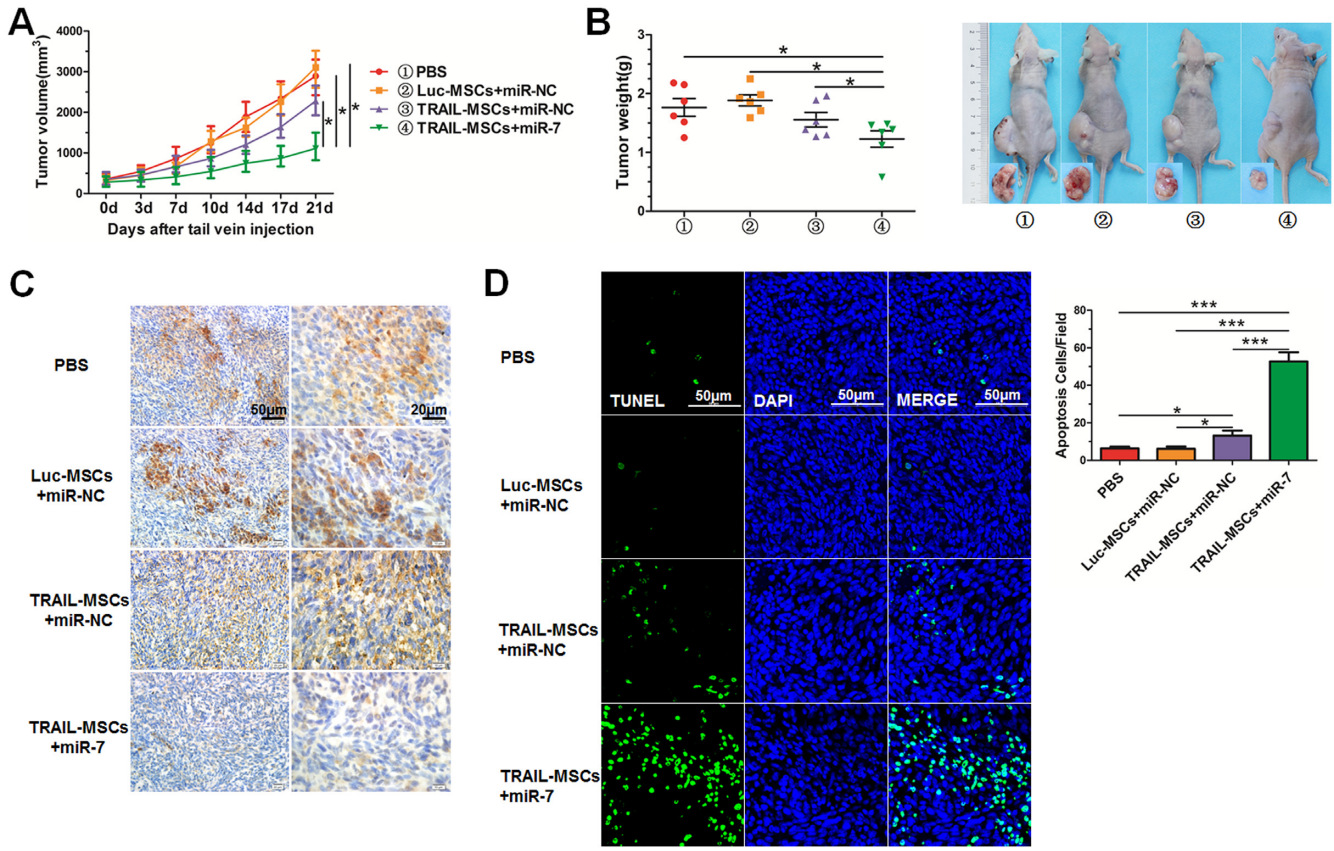

Figure 7. TRAIL and miR-7 combined expressing MSCs suppress tumor growth *in vivo*. (**A**) Graphical representation of the changes in the tumor volume ($n = 6$ per group) followed by tail vein injection of different modified MSCs for a period of 3 weeks. (**B**) Tumor weight of the excised tumors from the different treatment sets (left panel), Representative tumor sizes in different groups (right panel). (**C**) IHC analysis depicting the changes of XIAP expression level in excised tumors from the aforementioned sets using anti-XIAP antibody. (**D**) TUNEL staining assay showing the apoptotic cells of the excised tumors. Apoptotic cancer cells were averaged in six random fields each group. $*P < 0.05$, $***P < 0.001$; one-way ANOVA, mean ± SD, $n = 6$.

ability to specifically kill cancer cells, with slight effects on normal cells, and induces apoptosis by interacting with specific receptors (DR4 and DR5) (8). Current clinical trials using systemic administration of TRAIL or TRAIL receptor agonists have largely been unsuccessful revealed the importance of TRAIL resistance, even when these targeted drugs are known to penetrate into tumor tissues (5–7,32–35). This indicates that some inherent defects limit its utilization in the clinical application (36).

TRAIL displays a short half-life making it difficult to maintain therapeutically efficacious levels in the vicinity of tumor tissues (8). One strategy to overcome this challenge is to genetically modify TRAIL in MSCs. MSCs have been demonstrated to be a promising vehicle for delivering therapeutic agents to tumor tissues because of its tumor tropism. The effective delivery by MSCs overcomes some of the hurdles of conventional TRAIL-based treatments and achieves better apoptosis-inducing activity because of the highly local concentration of TRAIL around cancer cells. It has been reported that MSCs could penetrate the brain and infiltrate intracranial glioma xenografts in a mouse model (37–40). However, it does not tackle the intrinsic resistance of GBM cells to TRAIL.

MiRNAs are emerging as key regulators of multiple pathways involved in cancer development and progression, and may become the next targeted therapy in malignant diseases. The miRNA-based therapeutics has been validated in multiple types of cancer, including GBM (41). In recent years, a series of miRNAs has been demonstrated to play important roles in negatively regulating TRAIL sensitivity in GBM cells (42,43). They impair TRAIL-dependent apoptosis by inhibiting the expression of key functional proteins. For example, miR-21 suppresses TRAIL sensitivity in GBM cells by targeting a p53 family member TAp63. And miR-30 inhibits TRAIL responsiveness through inhibition of caspase-3 activation in GBM cells (43). And *in vivo* experiment showed that with the utilization of locked nucleic acid-anti-miR-21 oligonucleotides and neural precursor cells expressing TRAIL, this combinational approach leads to a synergistic effect on regression of tumor growth (42). However, even nowadays, there is no systematic screening for miRNA-based natural sensitizers for TRAIL-induced apoptosis in GBM cells. In the current study, using a global analysis in TRAIL sensitive and resistant GBM cells, we identified that miR-7, a tumor suppressor small non-coding RNA could be a potential sensitizer for TRAIL in GBM cells. Our gain and loss of function experiments validated that overexpression of miR-7 increases TRAIL sensitivity in resistant GBM cells, whereas miR-7 inhibition significantly decreases responsiveness of GBM cells to

TRAIL treatment. Moreover, we also provided evidences that this effect is not restricted to GBM, but also present in other types of cancer such as HCC cells. MiR-7 was previously reported to function as a tumor suppressor in GBM by directly targeting oncogenic molecules as EFGR, AKT1, IRS-1 and IRS-2 (44). Recently, we found that CCNE1 is a novel target of mir-7 controlling the cell cycle in HCC cells (45). As a brain enriched miRNA, we suppose that miR-7 could be a multifaceted molecular regulating multiple signaling pathways under physiological and pathological conditions. Here, we demonstrated that miR-7 is a natural sensitizer for TRAIL in GBM cells for the first time.

When we wonder to know the detailed molecular mechanism of miR-7′s effect on TRAIL sensitivity in GBM cells, we found that an IAP family member XIAP is a direct target gene of miR-7. XIAP blocks apoptosis downstream of mitochondria by binding to and inhibiting caspase-3 and caspase-9 (26,27). An increasing number of clinical trials of XIAP targeted cancer treatment further confirmed that XIAP is a node molecule regulating cell death sensitivity (46,47). Moreover, the results of our gene silencing and rescue experiments support the opinion that miR-7-XIAP axis contributes to TRAIL sensitivity in GBM and other types of cancer cell lines. Previous studies showed that in pancreatic cancer cells, RNAi-mediated inhibition of XIAP significantly enhanced TRAIL-induced apoptosis (48–50). However, to pretreat cancer cells with XIAP siRNAs and then induce cell death with TRAIL is not feasible for the clinic (51). A practical application should be established.

In recent years, a growing number of evidences demonstrated that exosomes could be a naturally delivery tool to transfer miRNAs for cell–cell communication (12–14). Zhang *et al*. showed that the monocyte-derived miR-150 facilitates migration of endothelial cell in an exosome-dependent manner (13). In EBV-infected B cells, that viral miRNAs are secreted from infected B cells and are functional upon transfer via exosomes in primary MoDC. EBV-miRNAs are present in non-infected non-B cells and consequently regulate immunological reactions by targeting its downstream genes (52), suggesting that functional miRNA transfer by exosomes is a possible mechanism of intercellular communication. All reports support that cells can secrete miRNAs and deliver them into recipient cells where the exogenous miRNAs can regulate target gene expression and recipient cell function. In our study, we speculated that enforced expression of exogenous miR-7 in sTRAIL-overexpressed MSCs may increase apoptosis and suppressed tumor growth in an exosome dependent manner. Finally, our proof-of-principle study showed that therapeutic miR-7 produced in MSCs and loaded into extracellular exosomes could lead to synergistic antitumor efficacy with sTRAIL by inhibiting its target gene XIAP. Although there is a significant decrease in tumor growth with the use of miR-7 and TRAIL-loaded MSCs, there was still tumor growth. To further increase therapeutic response, more potential miRNAs involved in regulation of TRAIL sensitivity should be identified and the MSCs-based treatment process should be optimized. Finally, our results imply that selective miRNA antagonism might allow for sensitizing GBM and other tumors for TRAIL-MSCs-based therapy and could thus be of considerable interest for development of novel GBM therapies.

SUPPLEMENTARY DATA

Supplementary Data are available at NAR Online.

ACKNOWLEDGEMENTS

The authors thank Wen-Jing Luo and Dan Li for the help on Live cell imaging system analysis provided by Department of Preventive Medicine, The Fourth Military Medical University.

FUNDING

National Natural Science Foundation of China [81630069 to A.Y., 81572763 to R.Z., 81502670 to X.Z., 81101710 to S.H., 31471044 to M.Z., 81421003 to K.W.]; National High Technology Research and Development Program (‘863’ Program) of China [2015AA020918 to M.Z.]. Funding for open access charge: National Natural Science Foundation of China [81572763].
Conflict of interest statement. None declared.

REFERENCES

1. Wadajkar,A.S., Dancy,J.G., Hersh,D.S., Anastasiadis,P., Tran,N.L., Woodworth,G.F., Winkles,J.A. and Kim,A.J. (2016) Tumor-targeted nanotherapeutics: overcoming treatment barriers for glioblastoma. *Wiley Interdiscip. Rev. Nanomed. Nanobiotechnol.*, doi:10.1002/wnan.1439.
2. Shah,K. (2016) Stem cell-based therapies for tumors in the brain: are we there yet? *Neuro. Oncol.*, **18**, 1066–1078.
3. Johnstone,R.W., Frew,A.J. and Smyth,M.J. (2008) The TRAIL apoptotic pathway in cancer onset, progression and therapy. *Nat. Rev. Cancer*, **8**, 782–798.
4. Walczak,H., Miller,R.E., Ariail,K., Gliniak,B., Griffith,T.S., Kubin,M., Chin,W., Jones,J., Woodward,A., Le,T. *et al.* (1999) Tumoricidal activity of tumor necrosis factor-related apoptosis-inducing ligand *in vivo*. *Nat. Med.*, **5**, 157–163.
5. Ashkenazi,A., Pai,R.C., Fong,S., Leung,S., Lawrence,D.A., Marsters,S.A., Blackie,C., Chang,L., McMurtrey,A.E., Hebert,A. *et al.* (1999) Safety and antitumor activity of recombinant soluble Apo2 ligand. *J. Clin. Invest.*, **104**, 155–162.
6. Ashkenazi,A., Holland,P. and Eckhardt,S.G. (2008) Ligand-based targeting of apoptosis in cancer: the potential of recombinant human apoptosis ligand 2/Tumor necrosis factor-related apoptosis-inducing ligand (rhApo2L/TRAIL). *J. Clin. Oncol.*, **26**, 3621–3630.
7. Herbst,R.S., Eckhardt,S.G., Kurzrock,R., Ebbinghaus,S., O’Dwyer,P.J., Gordon,M.S., Novotny,W., Goldwasser,M.A., Tohnya,T.M., Lum,B.L. *et al.* (2010) Phase I dose–escalation study of recombinant human Apo2L/TRAIL, a dual proapoptotic receptor agonist, in patients with advanced cancer. *J. Clin. Oncol.*, **28**, 2839–2846.
8. Stuckey,D.W. and Shah,K. (2013) TRAIL on trial: preclinical advances in cancer therapy. *Trends Mol. Med.*, **19**, 685–694.
9. Di Leva,G., Garofalo,M. and Croce,C.M. (2014) MicroRNAs in cancer. *Annu. Rev. Pathol.*, **9**, 287–314.
10. Garofalo,M., Quintavalle,C., Di Leva,G., Zanca,C., Romano,G., Taccioli,C., Liu,C.G., Croce,C.M. and Condorelli,G. (2008) MicroRNA signatures of TRAIL resistance in human non-small cell lung cancer. *Oncogene*, **27**, 3845–3855.
11. Garofalo,M., Di Leva,G., Romano,G., Nuovo,G., Suh,S.S., Ngankeu,A., Taccioli,C., Pichiorri,F., Alder,H., Secchiero,P. *et al.* (2009) miR-221&222 regulate TRAIL resistance and enhance tumorigenicity through PTEN and TIMP3 downregulation. *Cancer Cell*, **16**, 498–509.

12. Valadi,H., Ekström,K., Bossios,A., Sjöstrand,M., Lee,J.J. and Lötvall,J.O. (2007) Exosome-mediated transfer of mRNAs and microRNAs is a novel mechanism of genetic exchange between cells. *Nat. Cell Biol.*, **9**, 654–659.
13. Zhang,Y., Liu,D., Chen,X., Li,J., Li,L., Bian,Z., Sun,F., Lu,J., Yin,Y., Cai,X. *et al.* (2010) Secreted monocytic miR-150 enhances targeted endothelial cell migration. *Mol. Cell*, **39**, 133–144.
14. Melo,S.A., Sugimoto,H., O'Connell,J.T., Kato,N., Villanueva,A., Vidal,A., Qiu,L., Vitkin,E., Perelman,L.T., Melo,C.A. *et al.* (2014) Cancer exosomes perform cell-independent microRNA biogenesis and promote tumorigenesis. *Cancer Cell*, **26**, 707–721.
15. Miura,M., Chen,X.D., Allen,M.R., Bi,Y., Gronthos,S., Seo,B.M., Lakhani,S., Flavell,R.A., Feng,X.H., Robey,P.G. *et al.* (2004) A crucial role of caspase-3 in osteogenic differentiation of bone marrow stromal stem cells. *J. Clin. Invest.*, **114**, 1704–1713.
16. Zhang,X., Hu,S.J., Zhang,X., Wang,L., Zhang,X.F., Yan,B., Zhao,J., Yang,A.G. and Zhang,R. (2014) MicroRNA-7 arrests cell cycle in G1 phase by directly targeting CCNE1 in human hepatocellular carcinoma cells. *Biochem. Biophys. Res. Commun.*, **443**, 1078–1084.
17. Lu,Y., Liu,L., Wang,Y., Li,F., Zhang,J., Ye,M.X., Zhao,H., Zhang,X., Zhang,M., Zhao,J. *et al.* (2016) siRNA delivered by EGFR-specific scFv sensitizes EGFR-TKI-resistant human lung cancer cells. *Biomaterials*, **76**, 196–207.
18. Valadi,H., Ekström,K., Bossios,A., Sjöstrand,M., Lee,J.J. and Lötvall,J.O. (2007) Exosome-mediated transfer of mRNAs and microRNAs is a novel mechanism of genetic exchange between cells. *Nat. Cell Biol.*, **9**, 654–659.
19. Chen,B.B., Cao,H., Chen,L., Yang,X., Tian,X., Li,R. and Cheng,O. (2016) Rifampicin attenuated global cerebral ischemia injury via activating the nuclear factor erythroid 2-related factor pathway. *Front. Cell. Neurosci.*, **10**, 273.
20. Wang,L., Zhang,X., Jia,L.T., Hu,S.J., Zhao,J., Yang,J.D., Wen,W.H., Wang,Z., Wang,T., Zhao,J. *et al.* (2014) c-Myc-Mediated epigenetic silencing of MicroRNA-101 contributes to dysregulation of multiple pathways in hepatocellular carcinoma. *Hepatology*, **59**, 1850–1863.
21. Krek,A., Grün,D., Poy,M.N., Wolf,R., Rosenberg,L., Epstein,E.J., MacMenamin,P., da Piedade,I., Gunsalus,K.C., Stoffel,M. and Rajewsky,N. (2005) Combinatorial microRNA target predictions. *Nat. Genet.*, **37**, 495–500.
22. Bartel,D.P. (2009) MicroRNAs: target recognition and regulatory functions. *Cell*, **136**, 215–233.
23. Mi,H., Guo,N., Kejariwal,A. and Thomas,P.D. (2007) PANTHER version 6: protein sequence and function evolution data with expanded representation of biological pathways. *Nucleic Acids Res.*, **35**, D247–D252.
24. Chaturvedi,R., Asim,M., Piazuelo,M.B., Yan,F., Barry,D.P., Sierra,J.C., Delgado,A.G., Hill,S., Casero,R.A. Jr, Bravo,L.E. *et al.* (2014) Activation of EGFR and ERBB2 by Helicobacter pylori results in survival of gastric epithelial cells with DNA damage. *Gastroenterology*, **146**, 1739–1751.
25. Michels,J., Kepp,O., Senovilla,L., Lissa,D., Castedo,M., Kroemer,G. and Galluzzi,L. (2013) Functions of BCL-X L at the Interface between cell death and metabolism. *Int. J. Cell Biol.*, **2013**, 705294.
26. Deveraux,Q.L., Takahashi,R., Salvesen,G.S. and Reed,J.C. (1997) X-linked IAP is a direct inhibitor of cell-death proteases. *Nature*, **388**, 300–304.
27. Takahashi,R., Deveraux,Q., Tamm,I., Welsh,K., Assa-Munt,N., Salvesen,G.S. and Reed,J.C. (1998) A single BIR domain of XIAP sufficient for inhibiting caspases. *J. Biol. Chem.*, **273**, 7787–7790.
28. Liu,S., Zhang,P., Chen,Z., Liu,M., Li,X. and Tang,H. (2013) MicroRNA-7 downregulates XIAP expression to suppress cell growth and promote apoptosis in cervical cancer cells. *FEBS Lett.*, **587**, 2247–2253.
29. Trajkovic,K., Hsu,C., Chiantia,S., Rajendran,L., Wenzel,D., Wieland,F., Schwille,P., Brügger,B. and Simons,M. (2008) Ceramide triggers budding of exosome vesicles into multivesicular endosomes. *Science*, **319**, 1244–1247.
30. Savina,A., Furlán,M., Vidal,M. and Colombo,M.I. (2003) Exosome release is regulated by a calcium-dependent mechanism in K562 cells. *J. Biol. Chem.*, **278**, 20083–20090.
31. Studeny,M., Marini,F.C., Dembinski,J.L., Zompetta,C., Cabreira-Hansen,M., Bekele,B.N., Champlin,R.E. and Andreeff,M. (2004) Mesenchymal stem cells: potential precursors for tumor stroma and targeted-delivery vehicles for anticancer agents. *J. Natl. Cancer Inst.*, **96**, 1593–1603.
32. Leong,S., Cohen,R.B., Gustafson,D.L., Langer,C.J., Camidge,D.R., Padavic,K., Gore,L., Smith,M., Chow,L.Q., von Mehren,M. *et al.* (2009) Mapatumumab, an antibody targeting TRAIL-R1, in combination with paclitaxel and carboplatin in patients with advanced solid malignancies: results of a phase I and pharmacokinetic study. *J. Clin. Oncol.*, **27**, 4413–4421.
33. Tolcher,A.W., Mita,M., Meropol,N.J., von Mehren,M., Patnaik,A., Padavic,K., Hill,M., Mays,T., McCoy,T., Fox,N.L. *et al.* (2007) Phase I pharmacokinetic and biologic correlative study of mapatumumab, a fully human monoclonal antibody with agonist activity to tumor necrosis factor-related apoptosis-inducing ligand receptor-1. *J. Clin. Oncol.*, **25**, 1390–1395.
34. Ciprotti,M., Tebbutt,N.C., Lee,F.T., Lee,S.T., Gan,H.K., McKee,D.C., O'Keefe,G.J., Gong,S.J., Chong,G., Hopkins,W. *et al.* (2015) Phase I imaging and pharmacodynamic trial of CS-1008 in patients with metastatic colorectal cancer. *J. Clin. Oncol.*, **33**, 2609–2616.
35. Forero-Torres,A., Shah,J., Wood,T., Posey,J., Carlisle,R., Copigneaux,C., Luo,FR., Wojtowicz-Praga,S., Percent,I. and Saleh,M. (2010) Phase I trial of weekly tigatuzumab, an agonistic humanized monoclonal antibody targeting death receptor 5 (DR5). *Cancer Biother. Radiopharm.*, **25**, 13–19.
36. de Miguel,D., Lemke,J., Anel,A., Walczak,H. and Martinez-Lostao,L. (2016) Onto better TRAILs for cancer treatment. *Cell Death Differ.*, **23**, 733–747.
37. Duebgen,M., Martinez-Quintanilla,J., Tamura,K., Hingtgen,S., Redjal,N., Wakimoto,H. and Shah,K. (2014) Stem cells loaded with multimechanistic oncolytic herpes simplex virus variants for brain tumor therapy. *J. Natl. Cancer Inst.*, **106**, dju090.
38. Martinez-Quintanilla,J., Bhere,D., Heidari,P., He,D., Mahmood,U. and Shah,K. (2013) Therapeutic efficacy and fate of bimodal engineered stem cells in malignant brain tumors. *Stem Cells*, **31**, 1706–1714.
39. Redjal,N., Zhu,Y. and Shah,K. (2015) Combination of systemic chemotherapy with local stem cell delivered S-TRAIL in resected brain tumors. *Stem Cells*, **33**, 101–110.
40. Sasportas,L.S., Kasmieh,R., Wakimoto,H., Hingtgen,S., van de Water,J.A., Mohapatra,G., Figueiredo,J.L., Martuza,R.L., Weissleder,R. and Shah,K. (2009) Assessment of therapeutic efficacy and fate of engineered human mesenchymal stem cells for cancer therapy. *Proc. Natl. Acad. Sci. U.S.A.*, **106**, 4822–4827.
41. Li,Y., Guessous,F., Zhang,Y., Dipierro,C., Kefas,B., Johnson,E., Marcinkiewicz,L., Jiang,J., Yang,Y., Schmittgen,T.D. *et al.* (2009) MicroRNA-34a inhibits glioblastoma growth by targeting multiple oncogenes. *Cancer Res.*, **69**, 7569–7576.
42. Corsten,M.F., Miranda,R., Kasmieh,R., Krichevsky,A.M., Weissleder,R. and Shah,K. (2007) MicroRNA-21 knockdown disrupts glioma growth *in vivo* and displays synergistic cytotoxicity with neural precursor cell delivered S-TRAIL in human gliomas. *Cancer Res.*, **67**, 8994–9000.
43. Quintavalle,C., Donnarumma,E., Iaboni,M., Roscigno,G., Garofalo,M., Romano,G., Fiore,D., De Marinis,P., Croce,C.M. and Condorelli,G. (2013) Effect of miR-21 and miR-30b/c on TRAIL-induced apoptosis in glioma cells. *Oncogene*, **32**, 4001–4008.
44. Kefas,B., Godlewski,J., Comeau,L., Li,Y., Abounader,R., Hawkinson,M., Lee,J., Fine,H., Chiocca,E.A., Lawler,S. and Purow,B. (2008) microRNA-7 inhibits the epidermal growth factor receptor and the Akt pathway and is down-regulated in glioblastoma. *Cancer Res.*, **68**, 3566–3572.
45. Fang,Y., Xue,J.L., Shen,Q., Chen,J. and Tian,L. (2012) MicroRNA-7 inhibits tumor growth and metastasis by targeting the phosphoinositide 3-kinase/Akt pathway in hepatocellular carcinoma. *Hepatology*, **55**, 1852–1862.
46. Schimmer,A.D., Estey,E.H., Borthakur,G., Carter,B.Z., Schiller,G.J., Tallman,M.S., Altman,J.K., Karp,J.E., Kassis,J., Hedley,D.W. *et al.* (2009) Phase I/II trial of AEG35156 X-linked inhibitor of apoptosis protein antisense oligonucleotide combined with idarubicin and cytarabine in patients with relapsed or primary refractory acute myeloid leukemia. *J. Clin. Oncol.*, **27**, 4741–4746.
47. LaCasse,E.C., Cherton-Horvat,G.G., Hewitt,K.E., Jerome,L.J., Morris,S.J., Kandimalla,E.R., Yu,D., Wang,H., Wang,W., Zhang,R. *et al.* (2006) Preclinical characterization of AEG35156/GEM 640, a

second-generation antisense oligonucleotide targeting X-linked inhibitor of apoptosis. *Clin. Cancer Res.*, **12**, 5231–5241.
48. Vogler,M., Durr,K., Jovanovic,M., Debatin,K.M. and Fulda,S. (2007) Regulation of TRAIL-induced apoptosis by XIAP in pancreatic carcinoma cells. *Oncogene*, **26**, 248–257.
49. Vogler,M., Walczak,H., Stadel,D., Haas,T.L., Genze,F., Jovanovic,M., Gschwend,J.E., Simmet,T., Debatin,K.M. and Fulda,S. (2008) Targeting XIAP bypasses Bcl-2-mediated resistance to TRAIL and cooperates with TRAIL to suppress pancreatic cancer growth *in vitro* and *in vivo*. *Cancer Res.*, **68**, 7956–7965.
50. Vogler,M., Walczak,H., Stadel,D., Haas,T.L., Genze,F., Jovanovic,M., Bhanot,U., Hasel,C., Möller,P., Gschwend,J.E. *et al.* (2009) Small molecule XIAP inhibitors enhance TRAIL-induced apoptosis and antitumor activity in preclinical models of pancreatic carcinoma. *Cancer Res.*, **69**, 2425–2434.
51. Mohr,A., Albarenque,S.M., Deedigan,L., Yu,R., Reidy,M., Fulda,S. and Zwacka,R.M. (2010) Targeting of XIAP combined with systemic mesenchymal stem cell-mediated delivery of sTRAIL ligand inhibits metastatic growth of pancreatic carcinoma cells. *Stem Cells*, **28**, 2109–2120.
52. Pegtel,D.M., Cosmopoulos,K., Thorley-Lawson,D.A., van Eijndhoven,M.A., Hopmans,E.S., Lindenberg,J.L., de Gruijl,T.D., Würdinger,T. and Middeldorp,J.M. (2010) Functional delivery of viral miRNAs via exosomes. *Proc. Natl. Acad. Sci. U.S.A.*, **107**, 6328–6333.